Pressure sensor with optofluidic configuration

Sergio Calixto,[1,*] Francisco J. Sanchez-Marin,[1] and Martha Rosete-Aguilar[2]

[1]Centro de Investigaciones en Optica, Loma del Bosque 115, Leon, Gto. c.p. 37150, Mexico

[2]Centro de Ciencias Aplicadas y Desarrollo Tecnologico, Universidad Nacional Autonoma de Mexico, Apartado Postal 70–186, D.F. c.p. 04510, Mexico

*Corresponding author: scalixto@cio.mx

Received 15 July 2008; revised 15 October 2008; accepted 6 November 2008; posted 6 November 2008 (Doc. ID 98839); published 4 December 2008

We present a new kind of compact, simple, and low cost optical pressure sensor. The physical principle on which the sensor is based, components, layout of the system, and characterization are described. The range of pressures in which the sensor works is from about 0.5 to 3 psi (1 psi = 6.895 kPa). © 2008 Optical Society of America

OCIS codes: 120.0120, 130.3990, 350.3950, 160.5470.

1. Introduction

Through the years optical elements have been made of hard, undeformable materials such as glass, crystals (e.g., ZnS), or metals to mention but a few. The characteristics of elements such as radius of curvature and refractive index remain fixed through the lifetime of the component. Modern applications of optical elements demand that characteristics of these elements should be changeable at will. These deformable elements could be as big as telescope mirrors [1–3] or as small as microlenses with sizes of a few hundred micrometers [4]. Application of small deformable lenses has been done in cellular telephones [5,6], personal digital assistants, and web cameras, for example.

Besides the application of microlenses, miniature optical devices are used as scanners [7], variable apertures [8], and sensors to measure physical quantities such as pressure [9–12], refractive index [13–17], humidity [18], and more [19]. These sensors are versatile and small. Unfortunately those based on fiber optics should be used with other optical and electronic components that raise the cost of the whole instrument (sensor + electronics) [20].

Here we propose a simple and small optical device to measure the pressure of a liquid. It is made of two fibers and a deformable membrane that forms a lens when it is under pressure. In Section 2 we discuss the physical principle under which the sensor works. Section 3 describes a theoretical development to show that a membrane under pressure has the profile of a convex lens. Section 4 describes the sensor layout, materials, and fabrication method. Section 5 deals with the lens testing methods. In Section 6 the experiments to calibrate the sensor through the light intensity versus pressure effect on the deformable lens are described. In Section 7 we comment and conclude.

2. Physical Principle

A lens is defined when parameters such as refractive index, thickness, radius, and diameter are given. The relation between the focal length (f) of the lens and the parameters is given by the lens maker's formula [21]:

$$\frac{1}{f} = (n_1 - n_m)\left\{\frac{1}{r_1} - \frac{1}{r_2} + \frac{(n_1 - n_m)t}{n_1 r_1 r_2}\right\}, \qquad (1)$$

where n_l and n_m are the refractive index of the lens and the medium, r_1 and r_2 are the radii of the lens surfaces, and t is the thickness of the lens. If we suppose $r_1 = \infty$ then a linear relation between f and r_2 is found.

0003-6935/08/356580-06$15.00/0

Figure 1 shows a series of diagrams made with an optical design program. These diagrams show the physical situation when a collimated beam of light is sent to a hollow plano–convex lens. We have supposed a lens with a thickness of 11 mm, diameter of 3 mm, and $r_1 = \infty$. The liquid that fills the hollow lens is water ($n_1 = 1.333$). The parameter in the diagrams is radius r_2. We notice that at the beginning ($r_2 = \infty$) light just traverses the optical element, and no focusing occurs. When r_2 diminishes, light is focused. The smaller the radius r_2, the more pronounced the focusing effect. As we will see in Section 3 a change in r_2 can be caused by increasing the pressure inside the cell. Besides this focusing phenomenon light energy density increases, at a particular plane situated less than the focal length, as r_2 decreases. This is the physical basis of the proposed optofluidic pressure sensor.

3. Theoretical Profile of the Lens Formed Under Pressure

In 1993 Sugiura and Morita [22] described a theoretical development about the profile of a liquid-filled lens when its volume changes. From an optical point of view, the lens considered is a plano–convex one. The plane side is rigid while the convex is a deformable membrane. Later (1996) Rawicz and Mikhailenko [23] developed the method further and permitted the inclusion of the actual pressures inside the lens. Other parameters included were the Poisson ratio and the thickness of the membrane used to fabricate the lens.

To calculate the profiles of the lens when pressure changes the following equation was used [22]:

$$z = \frac{w}{4T}(a^2 - r^2), \tag{2}$$

where z represents the abscissas, w is the pressure, $2a$ is the diameter of the lens (0.30 cm), and r is the ordinates. T is the absolute tension in the film and was calculated using the equation shown in [23], which is given by

$$\left(\frac{m}{h} - \frac{1}{h}\right)T^3 + mwT^2 + 0.04167w^2a^2 = 0, \tag{3}$$

where m is the Poisson ratio of the film (0.9) and h is the thickness of the film (0.015 cm).

Calculated lens profiles for pressures ranging from 0.1 to 2.0 psi (1 psi = 6.895 kPa) can be seen in Fig. 2(a). The shapes shown are sections of a paraboloid.

To find the radius of curvature (R) for each lens shown in Fig. 2(a), the maximum value of z is considered. This maximum value is the sagitta (s). Then, by using the relation

$$R = \frac{s^2 + a^2}{2s}, \tag{4}$$

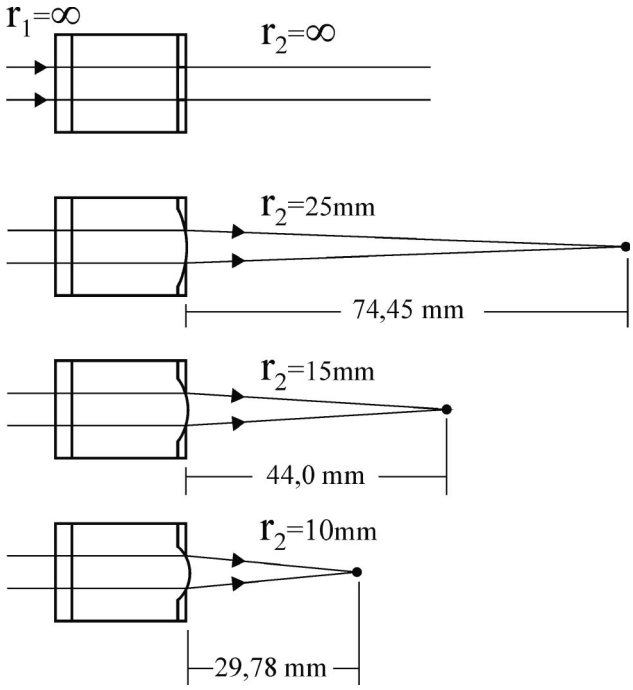

Fig. 1. Diagrams given by an optical design program of a plano–convex liquid-filled lens. The parameter is r_2, the radius of the membrane–lens under pressure. The lens concavity is not to scale. Note the focusing effect.

we find the radius of curvature of each lens. Focal distance is calculated with Eq. (1). The result is shown in Fig. 2(b). As can be seen, for low pressures the focal distance is long.

4. Liquid Cell Layout and Fabrication Method

The optical configuration in Fig. 3(a) shows the location of the different elements that compose the pressure sensor. A square (11 mm × 11 mm) plastic rim was used as a peripheral structure for the cell. Two circular apertures of about 3 mm were drilled, one on each side. A thin flat glass window was glued to one of them. A silicone thin membrane was glued to the other aperture.

The silicone that was used [24] is an elastomer that presents good flexibility and visible light transmittance, particularly in thin film form. It shows a refractive index of 1.4126. To make the membranes we chose the Doctor blade method [25]. Other methods (for example gravity settling) were tried, but it was not possible to make thin films because silicone shows high density. Several membranes were made with different arbitrary thicknesses of 150, 200, and 650 μm. To seal the cell at the bottom of the plastic rim a glass was glued to the rim. A thick (~1 mm) film of silicone was also glued to the top of the rim.

Light was sent to the cell by means of a fiber optic [Fig 3(b)]. The chosen fiber was a SM 600 (NA = 0.12) that is designed to work with red light from a He–Ne laser (632.8 nm). This fiber works in single mode. A plastic cone was used to fix the fiber. The fiber was inserted into the cone and then glued to it with the

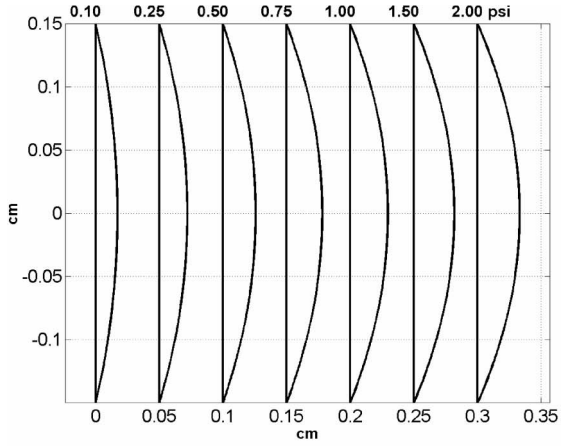

(a)

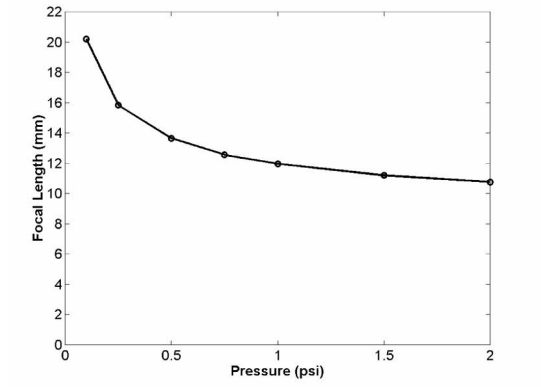

(b)

Fig. 2. (a) Theoretical profile of the liquid-filled lens for different pressures. (b) Theoretical focal length variation of the liquid-filled lens as a function of pressure.

same silicone mixture used to make the membrane. To collect the light focused by the membrane under pressure a multimode fiber with a core of 100 μm and a clad of 125 μm was chosen (i.e., a 100/125 fiber). This fiber was also inserted and glued into a plastic cone.

To ensure a perfect alignment of the fibers, with respect to the lens, the following method was used. $X-Y-Z$ micropositioners were used. First the incoming fiber was placed roughly in position. Then the fiber was moved with micropositioners until the spot of light illuminated the central part of the membrane. Next the plastic cone was glued. After this, the plastic cone of the outgoing fiber was put in the output aperture. This fiber was connected to a detector where intensity was measured. The fiber cone was moved with micropositioners until a maximum intensity was attained. Then the cone was glued.

The liquid used to fill the cell was distilled water. This process was done with the help of a syringe, and the needle was introduced through the silicone thick film. The pressure in the cell was increased by means of the piston of the syringe. Pressure was monitored by a gauge connected to the syringe.

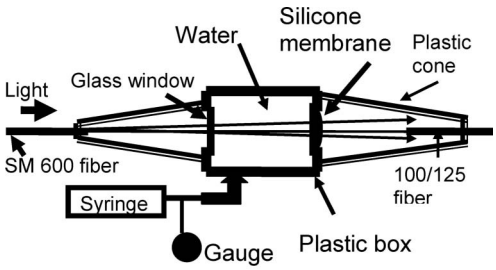

(a)

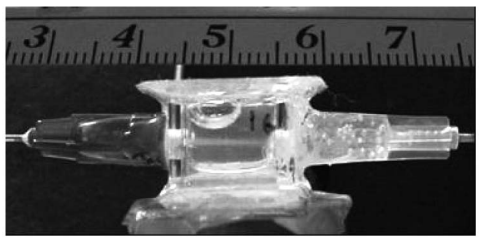

(b)

Fig. 3. (a) Diagram of the optical pressure sensor. (b) Photograph of one of the fabricated pressure sensors.

5. Testing the Lens

We have mentioned that the action of increasing the pressure in the cell implies the formation of a lens. With the help of an interference microscope we studied the surface of several membranes under pressure. It was found that some of them showed an irregular profile, Fig. 4(a), and others a good one, Fig 4(b). Lenses were also tested with the star test method [26]. To simulate the star we used a pinhole of about 400 μm as the light source. It was placed at about 2 m from the lens. Pinhole images given by the lenses were investigated with a low power microscope. One such image can be seen in Fig. 5(a). In this case the lens was formed under a pressure of 2.5 psi. The spot of light shows a round structure. In general the image of a point light source, or point spread function, has a very complex structure when aberrations are present [26]. Some of our lenses gave us nonsymmetrical images of point light sources with a nonuniform intensity. Thus, they were rejected, and those that gave a round image with a uniform spatial intensity were kept. The same lens that gave us the image in Fig. 5(a) was used to form an image of an object having three horizontal bars and three vertical bars of about 7 cm long by 1.5 cm wide. Also an asterisk of about 7 cm in diameter was used. These objects were placed at about 1 m from the lens and a pressure of 1 psi was applied. The image given by the lens is shown in Fig. 5(b). Note that the asterisk and bars are clear. The same lens also was used to form an image of a microscope. It was standing at about 1.5 m. The produced image is seen in Fig. 5(c). Also, some shelves can be seen.

Lenses were also tested to form images of near field objects. A U.S. Air Force (USAF) test target was placed at about 4 cm from the lens and a pressure of 2 psi was applied. The image given by the lens

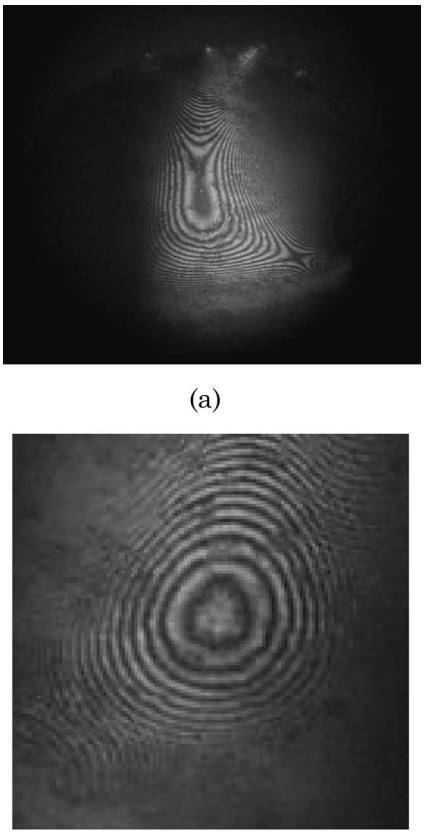

Fig. 4. Interference microscope views of the surface of two membranes under pressure. (a) Lens with irregular profile and (b) lens with a profile close to a sphere.

is shown in Fig. 5(d). In this figure it is possible to see that group 6, element 1 is resolved (64 line pairs/mm or 15.6 μm/line pair).

6. Pressure Measurements

With the help of an optical design software the membrane focusing effect was simulated. It was assumed that light leaving the SM 600 fiber was at 5 mm from the glass window. The angle of the cone of light was 7.3°, and the thickness of the cell was 11 mm. The diameter of the outgoing light cone was calculated at 8 mm from the membrane. At this distance the input face of the 100/125 fiber was placed. Several radii of curvature of the membrane (16–6 mm) were considered. Results can be seen in Fig. 6. The focusing effect is clearly seen. We point out that this simulation does not consider the thickness of the entrance window and the membrane. The thickness of each component is about 150 μm, which compared with the thickness of the cell (11 mm) is much smaller. In another set of calculations, considering the thickness, it was found that the diameter of the output beam changes by only 1.9% when $R = 16$ mm (Fig. 6). This change does not affect the calibration curve because calculations were used only as a guide.

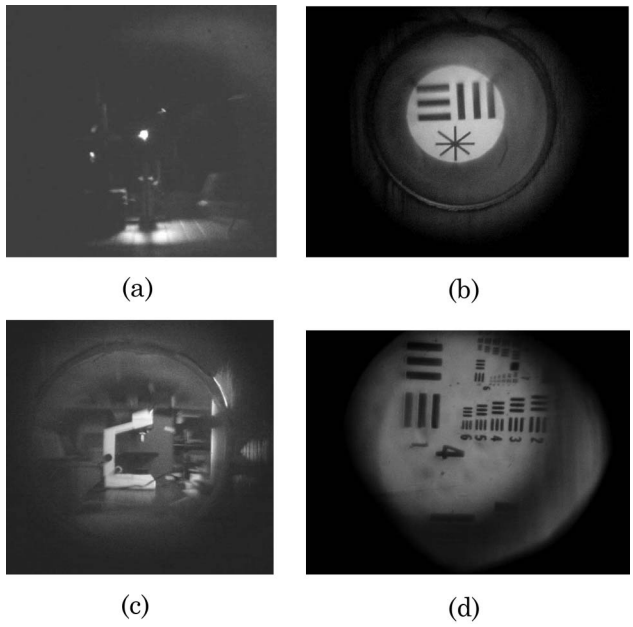

Fig. 5. Images of different objects given by a liquid-filled lens under pressure. Images were taken with a microscope. (a) Image of an illuminated pinhole (400 μm diameter), pressure 2.5 psi. (b) Image of an object with bars 7 cm × 1.5 cm. Object was at 1 m, pressure 1psi. (c) Image of a microscope. (d) Image of the USAF chart placed at 4 cm from the lens, pressure 2 psi.

A. Focal Distances

To find back focal distances of the lenses as a function of the pressure applied to the cell, an experiment was performed: an object was placed at 4 m from the lens, then a pressure was applied, and with the aid of a microscope the image plane was found. The distance from the lens to the plane was measured and considered as the back focal plane distance. The observed behavior is shown in Fig. 7(a), which also shows the theoretical curve of Fig. 2(b). As can be seen, the behavior of both curves is similar. We should not expect a perfect agreement of the curves due to the fact that polymers in their fabrication process suffer different manipulations, such as mixing of compounds, temperature changes, purity of the raw materials, and more. Such factors induce changes in the parameters of the silicone, such as the Poisson ratio, that affect the profile of the lens.

B. Characterization Curve

We have pointed out that the energy density of light at a given point after the membrane lens should increase when pressure in the cell increases. This is due to the focusing effect. An experiment was performed to test this statement. A He–Ne laser was left to stabilize for about half an hour. Water pressure (p) was increased by steps, and in every step light intensity leaving the 100/125 fiber was measured. This was done for several cells. An example of the obtained results is shown in Fig. 7(b). As expected, intensity increased as pressure increased. Software was used to determine the polynomial that gave the best fit to the set of experimental measurements.

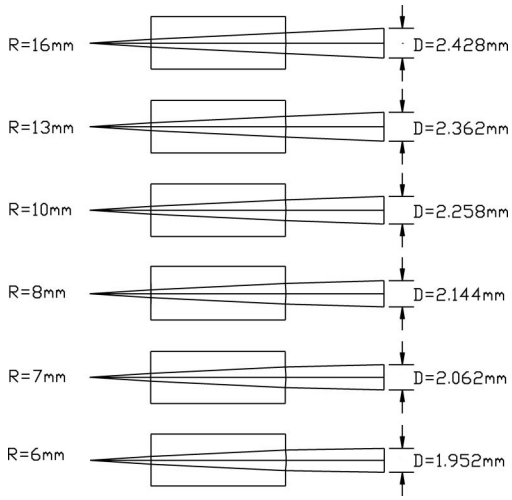

Fig. 6. Diagrams given by an optical design program. Light source at left was at 5 mm from the glass window. On the right, beam diameters are in a plane 8 mm from the membrane–lens.

The obtained formula is

$$I = 1.76527 + 0.52218\,p - 0.07273\,p^2. \qquad (5)$$

This curve also has been plotted in Fig. 7(b). With this polynomial the value of an unknown pressure could be calculated once the intensity of light has been measured.

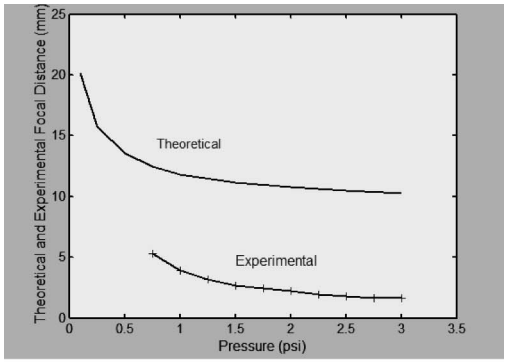

(a)

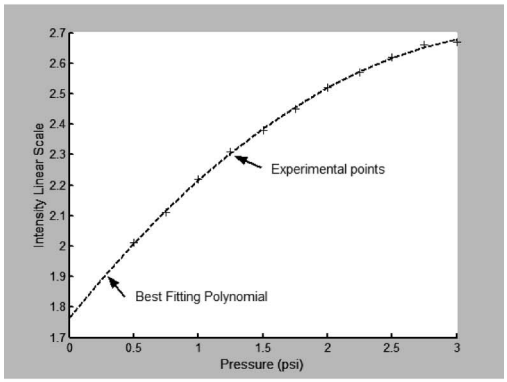

(b)

Fig. 7. (a) Theoretical and experimental focal distance versus pressure in the liquid-filled lens. (b) Light intensity after the liquid-filled lens versus pressure.

7. Comments and Conclusions

We have shown that it is possible to measure pressure in a liquid by means of a sensor that comprises a liquid-filled lens. This lens changes its curvature as pressure changes.

The pressure range in which the liquid-filled lens has been tested is between 0.5 and 3 psi (1 psi = 6.895 kPa). However, we foresee that this range can be changed if other liquids with different densities and refractive index and different membrane materials are used. This sensor is safe in hazardous environments—an attractive feature for those involved in, for example, the mining, aeronautics, or petrochemical industries—and the optical pressure sensor is simple, compact, and low cost. An advantage in using optical fibers is their immunity from all forms of electrical or magnetic interference.

References

1. A. B. Meinel and M. P. Meinel, "Inflatable membrane mirrors for opical passband imagery," Opt. Eng. **39**, 541–550 (2000).
2. E. F. Borra, "The case for liquid mirrors in orbiting telescopes," Astrophys. J. **373**, 317–321 (1991).
3. E. F. Borra, "The case for a liquid mirror in a lunar-based telescope," Astrophys. J. **392**, 375–383 (1992).
4. L. G. Commander, S. E. Day, and D. R. Selviah, "Variable focal length microlenses," Opt. Commun. **177**, 157–170 (2000).
5. S. Kuiper and B. H. W. Hendriks, "Variable-focus liquid lens for miniature cameras," Appl. Phys. Lett. **85**, 1128–1130 (2004).
6. www.varioptic.com. The site describes a liquid lens based on the electrowetting phenomenon.
7. A. N. Simonov, O. Akhzar-Mehr, and G. Vdovin, "Light scanner based on a viscoelastic stretchable grating," Opt. Lett. **30**, 949–951 (2005).
8. H. Yu, G. Zhou, S. F. Cau, and F. Lee, "Optofluidic variable aperture," Opt. Lett. **33**, 548–550 (2008).
9. J. Xu, X. Wang, K. L. Cooper, and A. Wang, "Miniature all-silica fiber optic pressure and acoustic sensors," Opt. Lett. **30**, 3269–3271 (2005).
10. X. Wang, J. Xu, Y. Zhu, K. L. Cooper, and A. Wang, "All fused-silica miniature optical fiber tip pressure sensor," Opt. Lett. **31**, 885–887 (2006).
11. K. Hosokawa, K. Hanada, and R. Maeda, "A polydimethylsiloxane deformable diffraction grating for monitoring of local pressure in microfluidic devices," J. Micromech. Microeng. **12**, 1–6 (2002).
12. www.fiso.com, FISO Technologies Inc., 500 St. Jean Baptiste Ave., Quebec, Canada.
13. V. Zamora, A. Diez, M. V. Andres, and B. Gimeno, "Refractometric sensor based on whispering-gallery modes of thin capillaries," Opt. Express **15**, 12011–12015 (2007).
14. P. Domachuk, I. C. M. Littler, M. Cronin-Golomb, and B. J. Eggleton, "Compact resonant integrated microfluidic refractometer," Appl. Phys. Lett. **88**, 093513 (2006).
15. S. Campopiano, R. Bernini, L. Zeni, and P. M. Sarro, " Microfluidic sensor based on integral optical hollow waveguides," Opt. Lett. **29**, 1894–1896 (2004).
16. E. Chow, Q. Grot, L. W. Mirkqrimi, M. Sigalas, and G. Girolami, "Compact biochemical sensor built with two-dimensional photonic crystal microcavity," Opt. Lett. **29**, 1093–1095 (2004).

17. S. Calixto, M. Rosete-Aguilar, D. Monzon-Hernandez, and V. P. Minkovich, "Capillary refractometer integrated in a microfluidic configuration," Appl. Opt. **47**, 843–848 (2008).
18. T. L. Yeo, T. Sun, and K. T. V. Grattan, "Fibre optic sensor technologies for humidity and moisture measurement," Sens. Actuators A **144**, 280–295 (2008).
19. C. Monat, P. Domachuk, and B. J. Eggleton, "Integrated optofluidics: A new river of light," Nat. Photonics **1**, 106–114 (2007).
20. J. Fraden, *Handbook of Modern Sensors: Physics, Designs and Applications* (Springer-Verlag, 1996).
21. M. Born and E. Wolf, *Principles of Optics* (Pergamon, 1975).
22. N. Sugiura and S. Morita,"Variable-focus liquid-filled optical lens," Appl. Opt. **32**, 4181–4186 (1993).
23. A. H. Rawicz and I. Mikhailenko, "Modeling a variable-focus liquid filled optical lens," Appl. Opt. **35**, 1587–1589 (1996).
24. Silastic T-2, Dow Corning Corp., South Saginaw Road, Midland, Michigan 48686, USA.
25. H. M. Smith, ed., *Holographic Recording Materials* (Springer-Verlag, 1977).
26. D. Malacara, ed., *Optical Shop Testing* (Wiley, 1978), Chap. 11.